



# Photoelectrochemical studies on electrodeposited indium doped CdSe thin films using aqueous bath



Vanita S. Raut<sup>a</sup>, Chandrakant D. Lokhande<sup>b</sup>, Vilas V. Killedar<sup>a,\*</sup>

<sup>a</sup> Department of Physics, Rajarshi Chhatrapati Shahu College, Kolhapur 416003 (MS), India

<sup>b</sup> Thin Film Physics Laboratory, Department of Physics, Shivaji University, Kolhapur 416004 (MS), India

## ARTICLE INFO

### Article history:

Received 4 January 2017

Received in revised form 4 February 2017

Accepted 7 February 2017

Available online 09 February 2017

### Keywords:

Thin film

Photoelectrochemical cell

Cadmium selenide

Electrochemical impedance spectroscopy

Indium doping

Band diagram

## ABSTRACT

Present investigation describes the photoelectrochemical studies of electrosynthesized CdSe and indium doped CdSe (In:CdSe) thin films deposited on stainless steel (SS) substrates. The photoelectrochemical (PEC) studies of both films are carried out with CdSe and In:CdSe(SS)/1 M Polysulfide/C cell. It is observed that indium doping in CdSe enhances the fill factor from 0.56 to 0.63 and photo-conversion efficiency from 0.80% to 2.01%. In order to study the consequence of doping, undoped and indium doped CdSe thin films are further characterized by capacitance-voltage, electrochemical impedance spectroscopy (EIS), spectral response, transient response, speed of response characterization techniques. By using capacitance-voltage measurement, various physical parameters are estimated and accordingly energy band diagrams have been constructed.

© 2017 Published by Elsevier B.V.

## 1. Introduction

The brisk growth of the world's energy demand from last several decades has brought substantial attention towards the energy scarcity problem [1]. To accomplish this ever-increasing energy demand mankind has been focused towards emerging renewable energy sources such as solar, nuclear, wind, tidal energy etc. Amongst these various renewable sources, solar energy is one of the best substitutes owing several rewards such as pollution free, abundantly available, inexhaustible and permanent source of energy. So, the nonstop conversion of solar energy into electrical energy is essential so as to accomplish the energy need of the present world. It is well known that photovoltaic devices are useful for solar energy conversion. These devices use p-n junction for direct conversion of solar energy into electrical energy. Due to simplicity in junction fabrication and inbuilt storage capacity, semiconductor liquid junction cells have attracted a great deal of interest over p-n junction solar cell [2]. The heart of efficient solar cell is photoelectrode (photocathode/photoanode) material, so appropriate selection of it is a crucial thing. The prime necessity while choosing photoelectrode material is its band gap energy, which should be expected to be positioned very close to visible spectrum maxima so as to make competent use of the solar energy spectrum. In this view, II–VI semiconductors have been a center of attention point because of sharp absorption edges, direct band gaps and higher absorption coefficient [3,4].

Cadmium selenide ( $E_g = 1.7$  eV) is one of the binary semiconductors from II–VI group which has fascinated attention of many researchers due to its interesting properties and wide range of applications [5–10]. Various chemical and physical methods have been employed for synthesis of CdSe thin films [11–16]. Increased optical absorption, decreased band gap plus resistivity of a photoelectrode material facilitate to achieve better and efficient performance in solar cell application. This can be done by doping photoelectrode material by suitable dopant like indium [17–24].

In the present investigation, the photoelectrochemical modifications arisen due to indium doping in potentiostatically electrosynthesized CdSe thin films are inspected. Further the effects of indium doping on the capacitance-voltage, band bending, electrochemical impedance spectroscopy, spectral response, speed of response and transient response characteristics of undoped and indium doped CdSe thin films is studied.

## 2. Experimental details

### 2.1. Synthesis of CdSe and indium doped CdSe (In:CdSe) thin films

The CdSe and In:CdSe thin films were potentiostatically electrodeposited on mirror polished stainless steel ( $5\text{ cm} \times 1\text{ cm} \times 0.05\text{ cm}$ ) and fluorine doped tin oxide (FTO) coated glass substrates (sheet resistance =  $15\ \Omega$ ) using three electrode cell. The cell was composed of three electrodes using substrate as a working electrode, graphite as a counter electrode and saturated calomel electrode as a reference electrode. All

\* Corresponding author.

E-mail address: [killedar\\_vilas@yahoo.co.in](mailto:killedar_vilas@yahoo.co.in) (V.V. Killedar).

the precursors used for deposition were analytical reagent grade and used without further purification. The  $\text{CdSO}_4$  used as cationic precursor,  $\text{SeO}_2$  used as anionic precursor and pH of the bath was maintained to  $3 \pm 0.1$ , using dilute  $\text{H}_2\text{SO}_4$ . Room temperature electrodeposition of CdSe thin film was carried out on well cleaned stainless steel substrates at deposition potential  $-0.59 \pm 0.01$  V/SCE, from the acidic aqueous bath containing 0.05 M  $\text{CdSO}_4$  (10 ml) and 0.01 M  $\text{SeO}_2$  (10 ml). The various preparative parameters used for electrodeposition of CdSe and In:CdSe thin films were optimized using the reliable photoelectrochemical (PEC) technique as published elsewhere [25]. The volumetric doping of indium (from 0.025 to 0.50 vol%) was carried out by adding up appropriate volumes of  $\text{InCl}_3$  solution in the electrolyte bath. The optimized volumetric doping percentage of indium was 0.15 vol%. Thus further studies were conducted with undoped and 0.15 vol% In:CdSe thin films.

## 2.2. Assembly and characterization of PEC cell

PEC cell was assembled using a two electrode system with pure CdSe or 0.15 vol% In:CdSe thin film as a photoanode and polished graphite as a counter electrode. 1 M Polysulfide (1 M NaOH–1 M  $\text{Na}_2\text{S}$ –1 M S) was used as a redox electrolyte. The photovoltaic power output characteristics were studied in dark and under constant illumination intensity of 50  $\text{mW}/\text{cm}^2$ . The area of photoanode exposed to illumination was 1  $\text{cm}^2$  other than that was enclosed by insulating tape, with the intention to put a stop on any other contribution to the net photocurrent density. A heat up problem of cell was solved by inserting a water lens between the lamp and PEC cell [26]. Here PEC cell was formed in an airtight container (to keep away oxygen from redox electrolyte) by direct dipping the CdSe or 0.15 vol% In:CdSe photoanode in polysulfide electrolyte.

## 2.3. PEC characterization

Photovoltaic power output characteristics, electrochemical impedance spectroscopy (EIS), spectral response, speed of response and transient response studies were carried out using two electrode system. The capacitance-voltage measurement was carried out using electrochemical workstation (ZIVE SP 5) with three electrode cell at a fixed frequency 1 kHz in the voltage range  $-0.8$  to  $0.8$  V. EIS studies of CdSe and In:CdSe thin film were performed in the frequency range 1 MHz to 100 mHz using same electrochemical workstation.

## 3. Results and discussion

Synthesis of CdSe and Indium doped CdSe thin films by the potentiostatic electrodeposition method has been confirmed using XRD and XPS analyses [25]. X-ray diffraction studies of both films confirmed cubic crystal structure with enhanced intensity of planes with indium doping. The XPS analysis confirmed the incorporation of indium in the CdSe thin film. Elemental composition studies showed undoped CdSe thin film is slightly cadmium rich while In:CdSe thin film contains average atomic percentage of Cd:In:Se elements as 54.89:1.30:43.81. Morphological modulation observed on introduction of indium. Nodules grown over the compact web of axial nanofibers like morphology observed, which found to be immensely useful for PEC cell application, as nodule helps to capture photons while nanofibers provides an easier electron transport path with better electrode-electrolyte contact. Wettability study signified more hydrophilic nature of In:CdSe thin film ensures more intimate contact between electrode and electrolyte. Optical absorption studies showed that indium doping causes decrease in band gap energy from 2.02 to 1.67 eV [25].

## 3.1. Photovoltaic power output characteristics and type of conductivity

As discussed earlier, PEC cell was formed with two electrode system containing CdSe or 0.15 vol% In:CdSe thin film as a photoanode, graphite as a counter electrode and 1 M polysulfide as redox electrolyte. Fig. 1 shows the J-V characteristics in dark and under illumination condition for pure CdSe and 0.15 vol% In:CdSe thin films. The current density-voltage (J-V) curves were recorded under fixed illumination intensity 50  $\text{mW}/\text{cm}^2$ . The PEC cell shows small current and voltage values in dark condition. The polarity of this current and voltage is found to be negative with respect to CdSe and 0.15 vol% In:CdSe electrode. The source of this voltage is accredited to variation in two half cell potentials of the PEC cell. Under illumination condition, open circuit voltage increases with negative polarity towards both CdSe and In:CdSe electrodes. This cathodic behavior of photovoltage towards CdSe and In:CdSe thin film, signifies that films have n-type conductivity [27].

The important parameters of PEC cell such as fill factor (FF) and power conversion efficiency ( $\eta$  %) are calculated using Eqs. (1) and (2) [2].

$$FF = \frac{I_m V_m}{I_{sc} V_{oc}} \quad (1)$$

where  $I_m$  and  $V_m$  be the maximum current and voltage that can be extracted from PEC cell while  $I_{sc}$  and  $V_{oc}$  represents short circuit current and open circuit voltage.

The relation for efficiency is,

$$\eta(\%) = \frac{I_m V_m}{P_{input}} \times 100 \quad (2)$$

Here,  $P_{input}$  is input power and product  $I_m V_m$  is maximum output power.

The series resistance,  $R_s$  and shunt resistance,  $R_{sh}$  are estimated from slope of output power characteristics using Eqs. (3) and (4)

$$\left(\frac{dI}{dV}\right)_{I=0} \cong \frac{1}{R_s} \quad (3)$$

$$\left(\frac{dI}{dV}\right)_{V=0} \cong \frac{1}{R_{sh}} \quad (4)$$

The values of  $I_{sc}$ ,  $V_{oc}$ ,  $I_m$ ,  $V_m$ , FF,  $\eta$ ,  $R_s$  and  $R_{sh}$  for pure and 0.15 vol% In:CdSe samples are tabulated in Table 1. For CdSe photoanode, the magnitude of  $I_{sc}$  and  $V_{oc}$  observed are 0.0016  $\text{A}/\text{cm}^2$  and 0.440 V, respectively. After indium doping these values are found to be enhanced to 0.0030  $\text{A}/\text{cm}^2$  and 0.512 V, respectively. Thus PEC cell performance

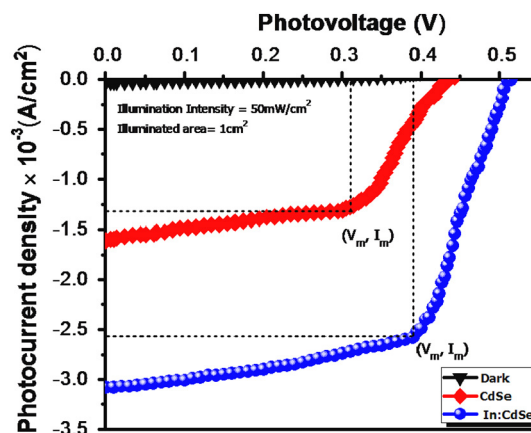


Fig. 1. Power output characteristics of CdSe and 0.15 vol% In:CdSe/1 M polysulfide/C PEC cells in dark and under illumination intensity of 50  $\text{mW}/\text{cm}^2$ .

**Table 1**  
Photoelectrochemical cell parameters of CdSe and 0.15 vol% In:CdSe photoanodes.

Sample	$I_{sc}$ (A/cm <sup>2</sup> )	$V_{oc}$ (V)	$I_m$ (A/cm <sup>2</sup> )	$V_m$ (V)	Fill factor	Efficiency (%)	$R_s$ ( $\Omega$ )	$R_{sh}$ ( $\Omega$ )
Pure CdSe	0.0016	0.440	0.0012	0.314	0.56	0.80	115	851
0.15 vol% In:CdSe	0.0030	0.512	0.0025	0.390	0.63	2.01	45	1821

was improved with indium doping. The efficiency and fill factor were boosted from 0.81% to 2.01% and 0.56 and 0.63, respectively as a consequence of indium doping. 0.15 vol% In:CdSe thin film shows superior performance than pure CdSe sample. This can be explained as, since open circuit voltage relies on height of potential barrier which is determined by the difference between fermi levels of photoanode and polysulfide electrolyte. Here the fermi level of redox electrolyte,  $E_{f_{redox}}$  is fixed using same electrolyte and the position of  $E_f$  semiconductor is altered varying indium doping percentage. Pure CdSe is n-type semiconductor whose cause is credited to selenium vacancies. Selenium vacancies act as donor centers while cadmium vacancies act as acceptor centers. Cadmium richness (selenium vacant) in CdSe sample generates donor levels below the conduction band edge. With indium doping, addition of  $In^{3+}$  to CdSe lattice creates donor levels in the band gap region. Thus doped indium increases donor concentration causing shift in fermi level position near to the conduction band, resulting in a decreased band gap [28]. Narrow band gap permits utilization of a more and more portion of the solar energy spectrum. This could be the reason for boosting PEC performance corresponding to 0.15 vol% indium doping, which is in good support with an optical study of the same [25].

### 3.2. Capacitance–voltage studies

The capacitance against applied potential measurement provides valuable information concerning flat band potential ( $V_{fb}$ ), donor density ( $N_D$ ), depletion region width ( $w$ ) and type of conductivity of the electrode under study. It helps to explain the characteristics of charge transport process taking place across the junction between semiconductor electrode and redox electrolyte of PEC cell.

The well-known Mott-Schottky relation [29] is,

$$\frac{1}{C_{sc}^2} = \frac{2}{q\epsilon_0\epsilon_s N_D} \left[ V - V_{fb} - \frac{k_B T}{q} \right] \quad (5)$$

where  $C_{sc}$  = space charge capacitance (F/m<sup>2</sup>),  $e$  = charge on an electron ( $1.6 \times 10^{-19}$  C),  $T$  = temperature (K),  $\epsilon_0$  = permittivity of free space =  $8.854 \times 10^{-12}$  F/m,  $\epsilon_s$  = relative permittivity of CdSe material = 10 [30],  $N_D$  = carrier density (m<sup>-3</sup>),  $V$  = applied potential,  $V_{fb}$  = flat band potential,  $k_B$  = Boltzmann constant ( $1.38 \times 10^{-23}$  J/K). The flat band potential is the intercept of the Mott-Schottky plot on potential axis at  $1/C_{sc}^2 = 0$ , while slope of Mott-Schottky plot is useful to calculate carrier density [31]. The Mott-Schottky (M-S) plots obtained for CdSe and 0.15 vol% In:CdSe photoanode/polysulfide electrolyte/graphite system at a fixed frequency of 1 kHz are shown in Fig. 2. The nonlinear nature of both Mott-Schottky plots (M-S plots) indicate formation of a graded junction between photoanode and redox electrolyte interface, which may be the consequence of surface coarseness, non-homogeneous doping, stacking faults originated due to spiky and uneven surface morphology, adsorption of ions on the surface of electrode etc. [32]. The flat band potential  $V_{fb}$  is found to be increased from  $-1.01$  to  $-1.19$  V/SCE upon indium doping, showing easier charge carrier transfer between doped CdSe nanofibers–electrolyte interface compared to undoped one [33]. This could be responsible for boosting up the PEC performance of 0.15 vol% In:CdSe thin film.

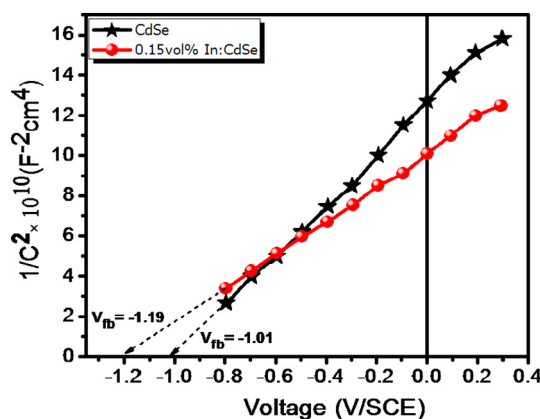


**Fig. 2.** Mott-Schottky plots for CdSe and 0.15 vol% In:CdSe photoanode/polysulfide PEC cells.

### 3.3. Estimation of band diagram and parameters evaluation from M-S plots

If the fermi level of redox electrolyte ( $E_{f_{redox}}$ ) and semiconductor electrode ( $E_f$ ) are known, then it is easy to evaluate the relative positions of valence band edge, conduction band edge, fermi level and extent of band bending.

As discussed earlier, slope of M-S plot enables to calculate the value of donor density  $N_D$ . The calculated values of donor density for CdSe and 0.15 vol% In:CdSe are  $1.04 \times 10^{16}$  and  $1.89 \times 10^{16}$  cm<sup>-3</sup>, respectively. Higher donor density values for doped CdSe electrode unambiguously avails additional charge carriers compared to undoped CdSe, which is favorable for easier electrical conduction process and it could be responsible for the enhanced PEC performance of the same.

The density of states in conduction band,  $N_c$  is calculated using Eq. (6).

$$N_c = \left( \frac{2}{h^3} \right) (2\pi m_e^* kT)^{1.5} \quad (6)$$

This is found to be equal to  $2.83 \times 10^{18}$  cm<sup>-3</sup>.

The relation of semiconductor Fermi level,  $E_f$  with  $N_c$  and donor density  $N_D$  is [29],

$$N_D = N_c \exp \left[ \frac{-(E_c - E_f)}{kT} \right] \quad (7)$$

Hence the energy separation between semiconductor conduction band edge and fermi energy, that is  $(E_c - E_f)$  is calculated using the relation,

$$(E_c - E_f) = -kT \ln \left[ \frac{N_D}{N_c} \right] \quad (8)$$

Using this relation, the values of  $(E_c - E_f)$  are found to be +0.15 and +0.13 V/SCE for CdSe and 0.15 vol% In:CdSe thin films respectively, which means the fermi levels of CdSe and 0.15 vol% In:CdSe are positioned +0.15 and +0.13 V/SCE lower than the conduction band, respectively. This outcome is probably due to additional donor level created by indium-doping. For indium doped CdSe electrode, fermi level is found to be more closely placed to conduction band as compared to undoped one. As in flat band situation, fermi level of semiconductor ( $E_f$ ) equals to flat band potential ( $V_{fb}$ ), therefore  $E_f$  for CdSe and In:CdSe corresponds to  $-1.01$  and  $-1.19$  eV/SCE, respectively. Thus the conduction band edge  $E_c$  of CdSe and 0.15 vol% In:CdSe electrode is found to be placed at  $-1.16$  and  $-1.32$  V/SCE, respectively.

The location of the valence band edge  $E_v$  can be projected, beneath the conduction band edge by the energy difference of the band gap

(estimated from the optical absorption study). Here the estimated band gap energies for CdSe and In:CdSe are 2.02 eV and 1.67 eV, respectively [25]. Thus, the locations of the valence band edge,  $E_v$  for CdSe and In:CdSe are at 0.86 and 0.35 V/SCE.

One of the important factors regarding the semiconductor electrode-redox electrolyte interface is band bending,  $V_{bb}$  which can be obtained by computing the difference between fermi levels of redox electrolyte (measured value of  $E_{f,redox} = -0.703$  V/SCE) [31] and electrode. In PEC cell, this fermi level difference is of immense importance as it directly gives an idea about the maximum value of photovoltage that can be obtained from the cell and thus helps in selection of appropriate electrolyte so as to acquire enhanced solar cell performance [2]. The band bending factor  $V_{bb}$  is found to be greater for 0.15 vol% In:CdSe (0.49) than CdSe (0.31). Increased band bending factor for 0.15 vol% In:CdSe is responsible for increased  $V_{oc}$ , which consequently liable for enhanced PEC cell performance compared to undoped CdSe. The barrier height,  $V_B$  is calculated using Eq. (9) as

$$V_B = qeV_{bb} + (E_c - E_f) \quad (9)$$

and is found to be 0.45 and 0.62 V corresponding to CdSe and 0.15 vol% In:CdSe electrode interfaces, respectively [34]. The energy band diagram thus built for CdSe and indium doped CdSe is shown in Fig. 3. The various physical parameters evaluated from Mott-Schottky (M-S) plots for CdSe and 0.15 vol% In:CdSe are listed in Table 2.

### 3.4. Electrochemical impedance spectroscopy (EIS) studies

In order to acquire additional information on the subject of charge transfer taking place across semiconductor-redox electrolyte interface, the EIS studies were carried out in the dark as well as under illumination condition. The PEC unit was composed of two electrode system. EIS studies performed using ZIVE workstation at room temperature in the frequency range 1 MHz to 100 mHz, by applying an AC potential to electrochemical system and consequently recording the shift in phase and amplitude of the resultant current response.

Impedance is a vector quantity with real part  $Z'$  and imaginary part  $Z''$  corresponding to the component in phase and with phase difference of  $90^\circ$  to cell voltage respectively. A plot of imaginary impedance component ( $Z''$ ) versus real impedance component ( $Z'$ ) is termed as Nyquist or Cole-Cole plot. Every point on the Nyquist plot stands for impedance at a particular frequency, where the left portion of the plot corresponds

**Table 2**

Various physical parameters of CdSe and 0.15 vol% In:CdSe thin films, calculated from the Mott-Schottky (M-S) plots.

Sr. No.	Samples → Physical parameters ↓	CdSe	0.15 vol% In:CdSe
1.	Flat band potential, $V_{fb}$ (V/SCE)	-1.01	-1.19
2.	Redox electrolyte	1 M polysulfide	1 M polysulfide
3.	Redox fermi potential, $E_{f,redox}$ (V/SCE)	-0.703	-0.703
4.	Donor density, $N_D$ ( $\text{cm}^{-3}$ )	$1.04 \times 10^{16}$	$1.89 \times 10^{16}$
5.	Density of states inside conduction band, $N_C$ ( $\text{cm}^{-3}$ )	$2.83 \times 10^{18}$	$2.83 \times 10^{18}$
6.	$E_c - E_f$ (eV/SCE)	0.15	0.13
7.	Conduction band boundary, $E_c$ (eV/SCE)	-1.16	-1.32
8.	Band bending, $V_{bb}$ (eV/SCE)	0.31	0.49
9.	Band gap energy, $E_g$ (eV)	2.02	1.67
10.	Valence band boundary, $E_v$ (eV/SCE)	0.86	0.35
11.	Barrier height, $V_B$	0.45	0.62
12.	Type of carrier	n-Type	n-Type

to higher frequencies, middle portion to middle frequencies and right portion corresponds to lower frequencies. Further, these impedance spectra are fitted to suitable electrical circuit with Zman software.

The recorded impedance spectra for CdSe and 0.15 vol% In:CdSe thin films in dark and under illumination conditions are shown in Fig. 4(a) and (b), respectively. Same electrical analog is fitted for all these spectra, as shown in Fig. 4(c). Fig. 4 enables to compare the changes in Nyquist plots in dark and upon illumination of PEC cell. Nyquist plot found to be largely influenced under illumination. Generally the PEC cell includes three different interfaces as stainless steel (SS) substrate/CdSe or In:CdSe photoanode, photoanode bulk/redox electrolyte and graphite/redox electrolyte. Thus, in the recorded impedance the key contribution is of photoanode side and very minor contribution from the graphite side. It was attained by maintaining more area of the graphite as compared to photoanode ( $1 \text{ cm}^2$ ) which reduces the interfacial resistance, thus affected less by a larger capacitance [35].

The impedance spectra for both photoanodes are best fitted to same electrical analog (Fig. 4c) containing a resistor R in series with two RC (sub circuit with  $R \parallel C$ ) circuits. For the better fit purpose the capacitances are replaced by constant phase elements Q1 and Q2. This equivalent circuit contains  $R_s$ ,  $R_1$ ,  $Q_1$ ,  $R_2$  and  $Q_2$  elements.  $R_s$  is the series resistance whose value corresponds to intercept on the real axis ( $Z'$ ) in the high frequency region, which arises due to the sheet resistance

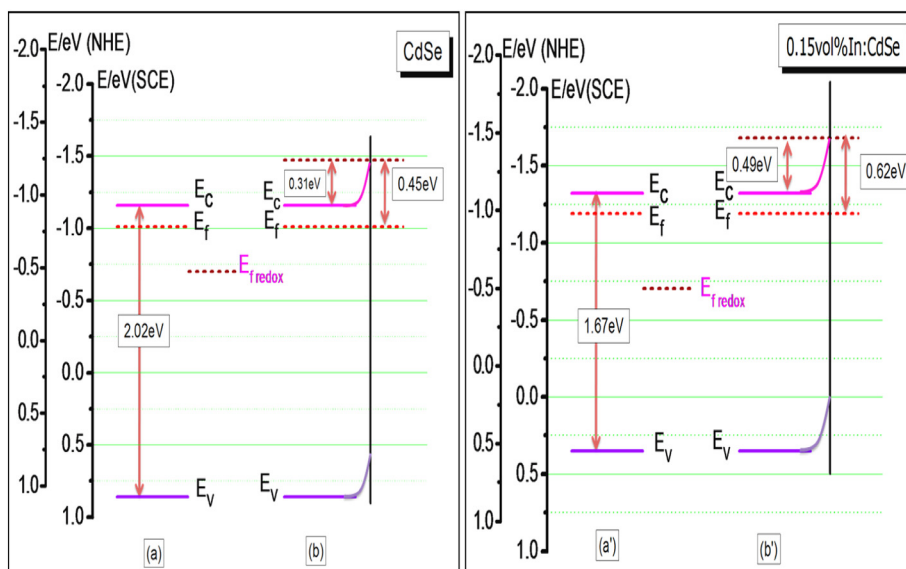


**Fig. 3.** The band diagrams of CdSe/polysulfide interface (a, b) and 0.15 vol% In:CdSe/polysulfide interface (a', b'): (a) and (a') at flat band condition, (b) and (b') band bending at the interface.

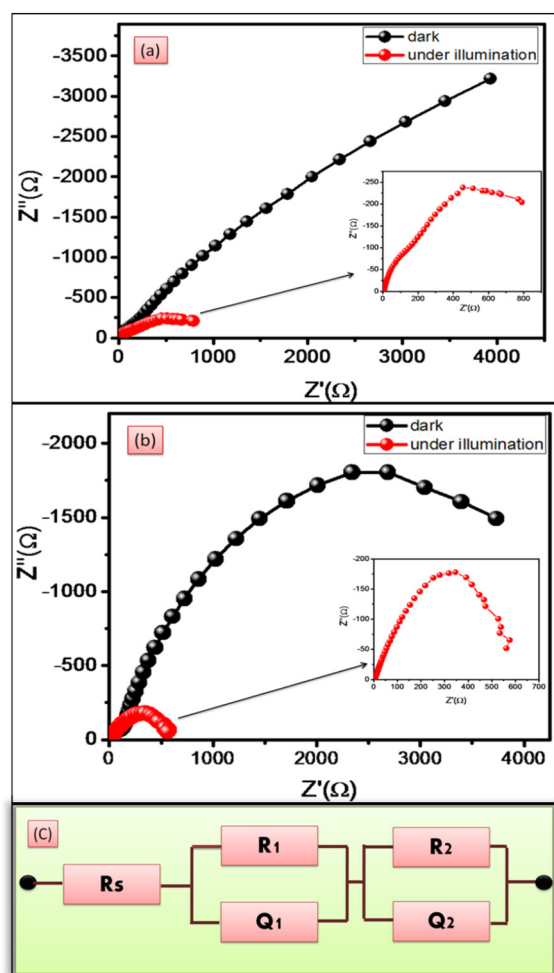


**Fig. 4.** Nyquist plots for CdSe (a) and 0.15 vol% In:CdSe (b) thin films in dark and under illumination condition and (c) an equivalent circuit diagram.

of the substrate, electrical resistivity of redox solution and exterior contact resistance (wire connections) of the PEC unit [36–38]. These two RC circuits can be allotted to photoanode bulk-substrate interface ( $R_1Q_1$ ) and Photoanode-electrolyte interface ( $R_2Q_2$ ). Thus,  $R_1$  and  $R_2$  are the charge transfer resistances at CdSe or 0.15 vol% In:CdSe photoanode-SS substrate interface and CdSe or 0.15 vol% In:CdSe photoanode-poly-sulfide electrolyte interface. While  $Q_1$  and  $Q_2$  are capacitances of substrate-photoanode interface (coupled with the non-uniform current allocation caused by roughness of photoanode material) and double layer at photoanode bulk electrolyte [39].

The values of electrical analog elements in dark and under illumination situation are listed in Table 3.  $R_s$  (is coupled with higher frequency reaction) shows no significant change upon illumination, specifying its

**Table 3**

Impedance parameters obtained from EIS analysis in dark and under illumination conditions.

Parameters	Samples			
	CdSe		0.15 vol% In:CdSe	
	Dark	Under illumination	Dark	Under illumination
$R_s$ ( $\Omega$ )	10.4	9.89	3.84	2.085
$R_1$ ( $\Omega$ )	18,387	1313	10,397	326
$Q_1$ (mF)	1.95	1.1	0.359	0.256
$R_2$ ( $\Omega$ )	3188	707.6	1044	179
$Q_2$ (mF)	0.074	0.16	0.298	0.564

independence on the same. As compared to dark situation, the charge transfer resistance ( $R_1$  and  $R_2$ ) corresponding to all charge transfer processes found to be incredibly low upon illumination. In the dark, when the electrode is dipped in an electrolyte, the charge equilibrium condition occurs by charge transfer and consequently accumulated charges are responsible for higher charge transfer resistance. While upon illumination, due to photoexcitation, conduction band electrons are able to flow through the circuit which lowers resistance. In dark  $Q_1$  is found to be greater than  $Q_2$ , which may be the consequence of the fact that the thickness of depletion layer is appreciably more than that of helmholtz layer thus depletion layer capacitance is smaller as compared to helmholtz layer capacitance [40]. Upon illumination  $Q_1$  decreases, screening uniform distribution of current all the way through bulk electrode. While  $Q_2$  found to be increased upon illumination, which is credited to accumulation of charges at the interfacial region (photogenerated electrons in bulk and holes near the surface of photoanode).

The In:CdSe photoanode exhibits lower charge transfer resistance and higher double layer capacitance compared to CdSe, which may be due to better photon capturing by nodules, easier electron transport path and better electrode electrolyte contact provided by an axial web of nanofibers. It confirms that indium doping enhances charge transfer, which could be responsible for the enhanced PEC performance of the same [25].

### 3.5. Spectral response

Spectral response study explicitly gives an idea regarding utilization of solar energy spectrum of the material under study. In this study the short circuit current ( $I_{sc}$ ) was recorded consequential to change in incident photon wavelength ( $\lambda$ ). Prior to that for a little time the PEC cell was kept in the dark and then study was undertaken with progression from larger to smaller wavelengths (from 850 to 450 nm). Fig. 5(a) shows the spectral response study of CdSe and 0.15 vol% In:CdSe/poly-sulfide/graphite PEC cells. Initially short circuit current found to be increased with wavelength, attains a maximum value at 700 and 600 nm for doped and undoped CdSe and declines for further increase wavelength for both electrodes. Decrease in short circuit current on smaller wavelength side is attributed to light absorption in redox electrolyte and surface recombinations of photogenerated minority charge carriers by surface states [9]. While decreased spectral response on larger wavelength side can be a consequence of poorer absorbance and higher transmittance of light. For In:CdSe PEC cell, the maxima of spectral response curve is found to be higher in magnitude and red shifted compared to undoped one. This increase in  $I_{sc}$  is accredited to the creation of indium donor levels and enlarged optical absorption, which may leads to improved PEC response for doped film. The short circuit current maxima is used to calculate energy band gap value. These maxima observed for CdSe and In:CdSe films are at 700 and 600 nm, respectively, which corresponds to an optical band gap of 1.77 and 2.06 eV. These band gap values are found to be in good agreement with that estimated (1.67 and 2.02 eV) from optical absorption studies [25,41].

### 3.6. Transient response

Fig. 5(b) shows transient response curves for CdSe and 0.15 vol% In:CdSe thin film PEC cells. Upon illumination PEC cell shows rise in photovoltage, which saturates after some time and upon exclusion of illumination, photovoltage decays. The rise in photovoltage is found to be instant while persistence of photovoltage has observed for some time after the cutoff of light excitation. This decay time that is the time taken by photovoltage to drop to its original value subsequent to the exclusion of light excitation is helpful to calculate decay constant and thus to study the charge transfer mechanism. Tentatively photovoltage decay curve can be split into three different sections related to high, intermediate and low level injection of minority carriers [42,43]. The log

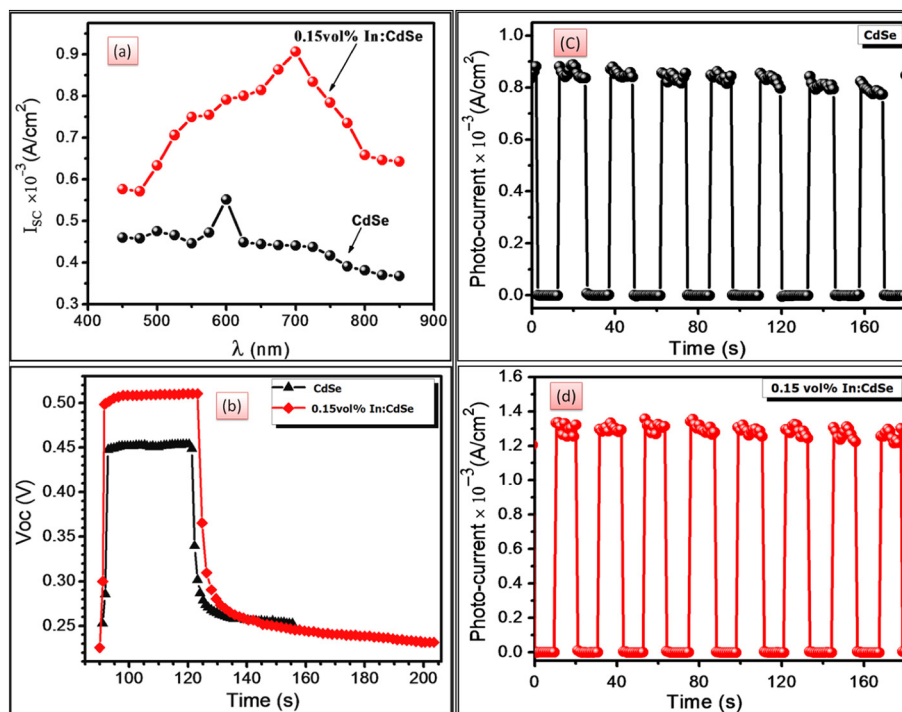


**Fig. 5.** (a) Spectral response curves of PEC cells formed with CdSe and 0.15 vol% In:CdSe photoanodes, (b) photoinduced voltage rise and decay curves for CdSe and 0.15 vol% In:CdSe/1 M polysulfide/C PEC cells, (c) and (d) represent the speed of response for CdSe and 0.15 vol% In:CdSe/1 M polysulfide/C PEC cells, respectively.

$V_{oc}$  versus time plot was found to be non-linear while the plot of  $\log V_{oc}$  versus  $\log t$  is linear obeying the equation [34].

$$V_{oc}(t) = V_{oc}(0)t^{-b} \quad (10)$$

where  $V_{oc}(0)$  and  $V_{oc}(t)$  represent open circuit voltages at time  $t = 0$  and  $t$  seconds while  $b$  is the decay constant. The slow decay in photovoltage is observed in the doped CdSe thin film compared to CdSe, ascribed to the presence of impurity levels and surface states in In:CdSe thin films. The decay constants obtained from the slope of  $\log V_{oc}$  versus  $\log t$  graph are found to be 0.63 and 0.43 for doped and undoped CdSe films, respectively.

### 3.7. Speed of response

Speed of response was tested for both indium doped and undoped CdSe thin film PEC cell over long time (180 s). In this study, the photo-current was recorded as a function of time under chopped light condition. Fig. 5(c) and (d) illustrate the speed of response study for undoped and indium doped CdSe thin films, respectively. It verifies continuous stability of thin film material for longer time duration, conquering the photocorrosion problem frequently observed in cadmium chalcogenides [44,45]. As well as, quick switching of current up and down under chopped light condition is an evidence of the photosensitive nature of materials, which recommends its use in device as a photosensor [46].

## 4. Conclusions

Thin films of CdSe and indium doped CdSe thin films have been synthesized using potentiostatic electrodeposition method. PEC studies reveal both CdSe and In:CdSe thin films possess n-type conductivity. The photo-conversion efficiency and fill factor are found to boost up from 0.80% to 2.01% and 0.56 to 0.63, respectively with indium doping. The flat band potentials obtained from the Mott-Schottky measurement found to be increased from  $-1.01$  to  $-1.19$  V/SCE with doping with indium. A band bending factor found to be enhanced from 0.31 to 0.49

after addition of indium. EIS studies show that indium doping lowers the charge transfer resistance, thus is beneficial for better charge transport process. Red shifted and the enhanced spectral response observed with indium incorporation in CdSe thin film.

## Acknowledgement

One of the authors (VSR) is indebted to UGC, New Delhi for the award of teacher fellowship. VSR is also grateful to the Secretary, Joint secretary of Rayat Shikshan Sanstha, Satara and Principal of A. M. A. and N.C.S. College, Rajapur for granting the study leave.

## References

- [1] M. Gratzel, Photoelectrochemical cells, *Nature* 414 (2001) 338–344.
- [2] C.D. Lokhande, S.H. Pawar, Electrochemical photovoltaic cells for solar energy conversion, *Mater. Chem. Phys.* 11 (1984) 201–277.
- [3] S.G. Kumar, K.S.R. Koteswara Rao, Physics and chemistry of CdTe/CdS thin film heterojunction photovoltaic devices: fundamental and critical aspects, *Energy Environ. Sci.* 7 (2014) 45–102.
- [4] T.L. Chu, S.S. Chu, Thin film II–VI photovoltaics, *Solid State Electron.* 38 (1995) 533–549.
- [5] F.Y. Gan, I. Shih, Preparation of thin-film transistors with chemical bath deposited CdSe and CdS thin films, *IEEE Trans. Electron Devices* 49 (2002) 15–18.
- [6] N.C. Greenham, X. Peng, A.P. Alivisatos, Charge separation and transport in conjugated-polymer/semiconductor-nanocrystal composites studied by photoluminescence quenching and photoconductivity, *Phys. Rev. B* 54 (1996) 17628–17637.
- [7] S. Mahato, A.K. Kar, Structural, optical and electrical properties of electrodeposited cadmium selenide thin films for applications in photodetector and photoelectrochemical cell, *J. Electroanal. Chem.* 742 (2015) 23–29.
- [8] B.O. Dabbousi, M.G. Bawendi, O. Onitsuka, M.F. Rubner, Electroluminescence from CdSe quantum-dot/polymer composites, *Appl. Phys. Lett.* 66 (1995) 1316–1318.
- [9] S.J. Lade, M.D. Uplane, C.D. Lokhande, Photoelectrochemical properties of CdX (X = S, Se, Te) films electrodeposited from aqueous and non-aqueous baths, *Mater. Chem. Phys.* 68 (2001) 36–41.
- [10] J.S. Jie, W.J. Zhang, Y. Jiang, S.T. Lee, Single-crystal CdSe nanoribbon field-effect transistors and photoelectric applications, *Appl. Phys. Lett.* 89 (1–3) (2006), 133118.
- [11] A.V. Shaikh, R.S. Mane, H.M. Pathan, B.K. Min, O.S. Joo, S.H. Han, CdSe thin film growth: primarily amorphous nanograins to self-assembled nanowires, *J. Electroanal. Chem.* 615 (2008) 175–179.
- [12] A. Zyouid, N.N. Abdul-Rahma, G. Campet, D. Park, H. Kwon, T.W. Kim, H.J. Choi, M.H.S. Helal, H.S. Hila, Enhanced PEC characteristics for CdSe polycrystalline film electrodes prepared by combined electrochemical/chemical bath depositions, *J. Electroanal. Chem.* 774 (2016) 7–13.

- [13] R. Choudhary, R.P. Chauhan, Gamma irradiation induced modifications in spin coated CdSe thin films, *J. Mater. Sci. Mater. Electron.* 27 (2016) 11674–11681.
- [14] S.A. Pawar, D.S. Patil, S.K. Patil, D.V. Awale, R.S. Devan, Y.R. Ma, S.S. Kolekar, J.H. Kim, P.S. Patil, Thiocyanate functionalized ionic liquid electrolyte for photoelectron chemical study of cadmium selenide pebbles, *Electrochim. Acta* 148 (2014) 310–316.
- [15] Y.P. Gnatenko, P.M. Bukivskij, I.O. Faryna, A.S. Opanasyuk, M.M. Ivashchenko, Photoluminescence of high optical quality CdSe thin films deposited by close-spaced vacuum sublimation, *J. Lumin.* 146 (2014) 174–177.
- [16] K.R. Murali, V. Subramanian, N. Rangarajan, Brush plated CdSe films and their photoelectrochemical characteristics, *J. Electroanal. Chem.* 368 (1994) 95–100.
- [17] Kriti Sharma, Alaa S. Al-Kabbi, G.S.S. Saini, S.K. Tripathi, Indium doping induced modification of the structural, optical and electrical properties of nanocrystalline CdSe thin films, *J. Alloys Compd.* 564 (2013) 42–48.
- [18] A.M. Perez Gonzalez, I.V. Arreola, C.S. Tepantlan, Effects of indium doping on the structural and optical properties of CdSe thin films deposited by chemical bath, *Rev. Mex. Fis.* 55 (2009) 51–54.
- [19] S. Alaa, Kriti Sharma Al-Kabbi, G.S.S. Saini, S.K. Tripathi, Effect of doping on trapping center parameters in nanocrystalline CdSe thin films, *J. Alloys Compd.* 555 (2013) 1–5.
- [20] C.K. Knox, S.D. Fillmore, D.M. Call, D.G. Allen, B.C. Hess, R.C. Davis, W.E. Evenson, R.G. Harrison, Synthesis and characterization of photo luminescent In-doped CdSe nanoparticles, *J. Colloid Interface Sci.* 300 (2006) 591–596.
- [21] Z. He, W. Zhang, W. Zhang, J. Jie, L. Luo, G. Yuan, J. Wang, C.M.L. Wu, I. Bello, C.-S. Lee, S.-T. Lee, High-performance CdSe:In nanowire field-effect transistors based on top-gate configuration with high-k non-oxide dielectrics, *J. Phys. Chem. C* 114 (2010) 4663–4668.
- [22] T. Hayashi, R. Saeki, T. Suzuki, M. Fukaya, Y. Ema, Formation and properties of In doped high conductivity CdSe evaporated film, *J. Appl. Phys.* 68 (1990) 5719–5723.
- [23] A.A. Yadav, E.U. Masumdar, Photoelectrochemical performances of indium-doped CdS<sub>0.2</sub>Se<sub>0.8</sub> thin film electrodes prepared by spray pyrolysis, *Electrochim. Acta* 56 (2011) 6406–6410.
- [24] P.A. Chate, P.P. Hankare, D.J. Sathe, Effect of indium doping on (CdZn)Se composite thin films, *J. Alloys Compd.* 505 (2010) 259–263.
- [25] V.S. Raut, C.D. Lokhande, V.V. Killedar, Synthesis and studies on effect of indium doping on physical properties of electrodeposited CdSe thin films, *J. Mater. Sci. Mater. Electron.* (2016) <http://dx.doi.org/10.1007/s10854-016-5902-6>.
- [26] R.N. Pandey, K.S. Chandra babu, O.N. Srivastava, High conversion efficiency photoelectrochemical solar cells, *Prog. Surf. Sci.* 52 (1996) 125–192.
- [27] V.V. Killedar, C.D. Lokhande, C.H. Bhosale, (Photo)electrochemical studies on spray deposited Sb<sub>2</sub>S<sub>3</sub> thin films from non-aqueous media, *Indian J. Pure Appl. Phys.* 36 (1998) 33–37.
- [28] C.D. Lokhande, S.H. Pawar, Effect of aluminium doping on properties of PEC cells formed with CdS:Al films, *Mat. Res. Bull.* 18 (1983) 1295–1301.
- [29] K.Y. Rajpure, C.H. Bhosale, A study of substrate variation effects on the properties of n-Sb<sub>2</sub>S<sub>3</sub> thin film/polyiodide/C photoelectrochemical solar cells, *Mater. Chem. Phys.* 64 (2000) 14–19.
- [30] M.A. Russak, J. Reichman, H. Witzke, S.K. Deb, S.N. Chen, Thin film CdSe photoanodes for electrochemical photovoltaic cells, *J. Electrochem. Soc.* 127 (1980) 725–733.
- [31] V.D. Das, L. Damodare, A study of band-bending and barrier height variation in thin film n-CdSe<sub>0.5</sub>Te<sub>0.5</sub> photoanode/polysulphide junctions, *Solid State Commun.* 99 (1996) 723–728.
- [32] A.B. Bhalerao, B.G. Wagh, N.M. Shinde, S.B. Jambure, C.D. Lokhande, Crystalline zinc indium selenide thin film electrosynthesis and its photoelectrochemical studies, *Energy Procedia* 54 (2014) 549–556.
- [33] S.J. Patil, V.C. Lokhande, D.-W. Lee, C.D. Lokhande, Electrochemical impedance analysis of spray deposited CZTS thin film: effect of Se introduction, *Opt. Mater.* 58 (2016) 418–425.
- [34] R.R. Sawant, S.S. Shinde, C.H. Bhosale, K.Y. Rajpure, Influence of substrates on photoelectrochemical performance of sprayed n-CdIn<sub>2</sub>S<sub>4</sub> electrodes, *Sol. Energy* 84 (2010) 1208–1215.
- [35] J.O.M. Bockris, A.K.N. Reddy, M. Gamboa-aldeco, *Modern Electrochemistry Fundamentals of Electrodeics*, second ed. Volume 2A, Springer, New York, 2008 1127–1138 (Chapter 7 – Electrodeics).
- [36] W. Ke, D. Zhao, A.J. Cimaroli, C.R. Grice, P. Qin, Q. Liu, L. Xiong, Y. Yan, G. Fang, Effects of annealing temperature of tin oxide electron selective layers on the performance of perovskite solar cells, *Mater. Chem. A* 3 (2015) 24163–24168.
- [37] Z. Huang, G. Natu, Z. Ji, P. Hasin, Y. Wu, P-type dye-sensitized NiO solar cells: a study by electrochemical impedance spectroscopy, *J. Phys. Chem. C* 115 (2011) 25109–25114.
- [38] R. Kern, R. Sastrawan, J. Ferber, R. Stangl, J. Luther, Modeling and interpretation of electrical impedance spectra of dye solar cells operated under open-circuit conditions, *Electrochim. Acta* 47 (2002) 4213–4225.
- [39] C. Longo, A.F. Nogueira, M.A. De Paoli, Solid-state and flexible dye-sensitized TiO<sub>2</sub> solar cells: a study by electrochemical impedance spectroscopy, *J. Phys. Chem. B* 106 (2002) 5925–5930.
- [40] T. Lopes, L. Andrade, H.A. Ribeiro, A. Mendes, Characterization of photoelectrochemical cells for water splitting by electrochemical impedance spectroscopy, *Int. J. Hydrog. Energy* 35 (2010) 11601–11608.
- [41] V.V. Killedar, C.D. Lokhande, C.H. Bhosale, (Photo)electrochemical studies on spray deposited Bi<sub>2</sub>S<sub>3</sub> thin films from non-aqueous media, *Indian J. Pure Appl. Phys.* 36 (1998) 643–647.
- [42] R.S. Mane, B.R. Sankapal, C.D. Lokhande, Photoelectrochemical (PEC) characterization of chemically deposited Bi<sub>2</sub>S<sub>3</sub> thin films from non-aqueous medium, *Mater. Chem. Phys.* 60 (1999) 158–162.
- [43] V.V. Killedar, K.Y. Rajpure, P.S. Patil, C.H. Bhosale, Transient photoconductivity measurements of spray deposited Sb<sub>2</sub>S<sub>3</sub> and Bi<sub>2</sub>S<sub>3</sub> thin films from non-aqueous medium, *Mater. Chem. Phys.* 59 (1999) 237–241.
- [44] S.S. Kale, U.S. Jadhav, C.D. Lokhande, Effect of Cd:S ratio on the photoconducting properties of chemically deposited CdS films, *Mater. Chem. Phys.* 69 (2001) 125–132.
- [45] G. Hodes, I. Howel, I. Peter, Nanocrystalline photoelectrochemical cells a new concept in photovoltaic cells, *J. Electrochem. Soc.* 139 (1992) 3136–3140.
- [46] V.V. Todkar, R.S. Mane, C.D. Lokhande, S.-H. Lee, S.-H. Han, Use of amorphous monodispersed spinel film electrode in photo-electrochemical cells, *Electrochim. Acta* 51 (2006) 4674–4679.